JOURNAL OF SOLID STATE CHEMISTRY 25, 285–294 (1978)

Crystallographic Studies on Cation Substitutions in the System (Na,K) (V,P)O_3

K. L. IDLER, C. CALVO,* AND H. N. NG†

Institute for Materials Research, McMaster University, 1280 Main St. W., Hamilton, Ontario L8S 4M1, Canada

Received November 8, 1977; in revised form January 23, 1978

Three compounds in the system (Na,K) (V,P)O_3 were synthesized and their structures were refined by full matrix least squares method in the space group $C2/c$. Their compositions were shown by site population analysis to be $Na(V_{0.66}P_{0.34})O_3$ (I), $(Na_{0.88}K_{0.12})VO_3$ (II), and $(Na_{0.5}K_{0.5})VO_3$ (III). All are related to the structure of α-$NaVO_3$ which in turn is related to the clinopyroxene structure characterized by infinite chains of SiO_4 tetrahedra sharing vertices and two inequivalent metal cation sites $M1$ and $M2$. Both sites feature sixfold coordination in compounds I and II, while the Na and K are ordered into $M1$ and $M2$ sites, respectively in III, with the latter showing eightfold coordination. The pentavalent cations are randomly distributed in tetrahedral sites in I, and in II the K was found to occupy the $M2$ sites only. Changes in the α-$NaVO_3$ structure upon cation substitution are discussed in terms of rotation and displacement of the tetrahedral chains. Parameters for measuring these chain movements are proposed and found to exhibit an almost linear relationship with the ratio $\langle X\text{–}0\rangle/\langle M2\text{–}0\rangle$ in cases where the $M1$ site is exclusively occupied by Na.

Introduction

The alkali metal metavanadates are structurally related to the group of minerals known as pyroxenes which are characterized by $(SiO_3)_\infty$ chains formed by vertex-sharing SiO_4 tetrahedra. In nature, the most common pyroxenes fall into two classes: the orthorhombic or orthopyroxenes and the monoclinic or clinopyroxenes. KVO_3, $RbVO_3$, and $CsVO_3$ (*1*), together with NH_4VO_3 (*1*) and $TlVO_3$ (*2*), are orthorhombic with the space group *Pbcm*. $NaVO_3$ (*3–5*) and $LiVO_3$ (*6*) are monoclinic with the modified diopside ($CaMgSi_2O_6$) structure, a prototype for clinopyroxenes. Both structures have been refined in the space group $C2/c$, but violation of the c-glide symmetry has been noted in the case of $LiVO_3$ and ferroelectric behavior below 380°C has been reported for $NaVO_3$ (*7, 8*).

As part of our overall structural studies on the pyroxene-like metavanadates, this work attempts to study the effect of cation substitutions on these monoclinic structures. Some cation substitution studies on the system (Na,K) (V,P)O_3 have been reported. Bergman and Sanzharova (*9*) found no compound formation between $NaVO_3$ and $NaPO_3$, but Ohashi (*10*) reported the existence of some mixed phases. Perraud (*11*), in his study of the $NaVO_3$–KVO_3 system, reported the existence of two monoclinic metavanadates, $(Na_{0.5}K_{0.5})VO_3$ and $(Na_{0.75}K_{0.25})VO_3$. Glazyrin (*12*), however, found only one compound at 50 mole% of KVO_3. It was also intended in this study to determine if ordering of V and P would occur resulting in the formation of two inequivalent tetrahedral chains,

* Deceased.

† Author to whom correspondence should be addressed.

0022–4596/78/0253–0285$02.00/00

and if the K and Na would order into the two independent cation sites as Ca and Mg do in the true diopside structure. Attempts were made to synthesize the compounds $Na(V_{0.67}P_{0.33})O_3$, $(Na_{0.75}K_{0.25})VO_3$, and $(Na_{0.5}K_{0.5})VO_3$. Subsequent site population analysis on the X-ray data of the synthesized crystals showed that they have the compositions $Na(V_{0.66}O_{0.34})O_3$, $(Na_{0.88}K_{0.12})VO_3$, and $(Na_{0.5}K_{0.5})VO_3$, hereafter referred to as compounds I, II, and III, respectively.

Experiments

Crystals of $Na(V_{0.66}P_{0.34})O_3$ (I) were grown from a mixture of $NaPO_3$, V_2O_5, and $Na_2CO_3 \cdot H_2O$ in the molar ratio of 1 : 1 : 1. The mixture was heated to 900°C in a Pt crucible and cooled at 6°C/hr to 500°C and was then quenched to room temperature. Crystals of $(Na_{0.88}K_{0.12})VO_3$ (II) were grown from a mixture of V_2O_5, $Na_2CO_3 \cdot H_2O$, and K_2CO_3 in a molar ratio of 4:3:1. It was heated to 600°C in a Pt crucible, held at 550°C for 2 days, and then quenched in air. $(Na_{0.5}K_{0.5})VO_3$ (III) was obtained from a melt containing equal molar amounts of KVO_3 and $NaVO_3$. It was cooled slowly from 560 to 400°C in a Pt crucible and then quenched in air. All the crystals are clear, colorless and needle-like. Crystals with dimensions 0.10 × 0.15 × 0.30 mm, 0.13 × 0.11 × 0.32 mm, and 0.06 × 0.06 × 0.35 mm for I, II, and III were used for intensity measurements.

Intensity data were collected on two Syntex automatic diffractometers, Model $P\bar{1}$ and $P2_1$. Graphite-monochromatized MoKα radiation (λ = 0.71069 Å) was used in the $\theta/2\theta$ scan mode. Variable scan rate from 8.0 to 24.0°/min in 2θ was used to minimize counting errors for the weak reflections. Accurate unit cell parameters were obtained by a least-squares refinement of the 2θ values ($20° < 2\theta < 40°$) of 15 reflections carefully measured on the diffractometer. Reflections within a sphere defined by $2\theta \leq 55°$ were collected. Subsequent averaging led to unique sets of 604, 486, and 732 reflections for I, II, and III, respectively. The data were corrected for Lorentz and polarization effects. Absorption correction was also applied in each case assuming cylindrical shape for the crystals. The crystal of II used for data collection was shown by precession photographs to be twinned. The twinning was found to correspond to a 180° rotation about a*. Intensity data were collected separately for the twin components, and a plot of the intensities of the twin-related reflections revealed a volume ratio of 4.7:1. Only the data for the major component were used. The intensities of the *hk*0 reflections, which are superposed because of twinning, were reduced by a factor of 4.7/5.7 before being used in the refinement.

Precession photographs showed that in each case the conditions of systematic absences were $h + k \neq 2n$ for *hkl* and $l \neq 2n$ for *h*0*l*. The centric space group $C2/c$ was chosen over the acentric Cc from a consideration of the statistical distribution of intensities. Long exposure showed no violation of the *c*-glide symmetry.

Structural Refinements

The first structure refined was that of $Na(V_{0.66}P_{0.34})O_3$. The positions of the cations were derived from Patterson functions. The positional parameters of the oxygen atoms were initially taken from those of α-$NaVO_3$. The final parameters from this refined structure of I were used as initial parameters for the other two. A full matrix least-squares program that minimizes the function $\sum w(|F_o| - |F_c|)^2$ was used. The weighting function used has the form $w = [A + B|F_o| + C|F_o|^2 + D(\sigma F_o|F_o)^2]^{-1}$ with the coefficients chosen in such a way that the averages of $w(\Delta F)^2$ were approximately constant when the data were analyzed into regions of F_o. In the case where two different cations may occupy the same site, the ratio of the two species was derived from their atomic numbers and the refined population parameter for that site,

TABLE I

CRYSTAL DATA[a]

	α-$NaVO_3$[b]	$Na(V_{0.66}P_{0.34})O_3$ (I)	$(Na_{0.88}K_{0.12})VO_3$ (II)	$(Na_{0.5}K_{0.5})VO_3$ (II)
a (Å)	10.552(3)	10.421(1)	10.533(2)	10.533(1)
b (Å)	9.468(2)	9.475(1)	9.580(2)	9.997(1)
c (Å)	5.879(2)	5.715(1)	5.850(1)	5.804(2)
β (deg)	108.47(3)	107.62(1)	107.56(1)	104.17(1)
V (Å^3)	557.1	537.8	562.8	592.6
Z	8	8	8	8
Space group	$C2/c$	$C2/c$	$C2/c$	$C2/c$
D_x (g/cm^3)	2.91	2.85	2.93	2.92

[a] Estimated standard deviations in parentheses.
[b] Reference (*4*).

using a scattering curve for the species with the larger proportion, e.g., that of Na in site $M2$ of II. During final stages of refinement, a secondary extinction parameter following Larson (*13*) was also refined. The crystal data for these three compounds are listed in Table I, together with those for $NaVO_3$ for comparison. Table II lists the weighting coefficients, the secondary extinction parameter g, the conventional residual R, and the weighted R factor R_w. Positional parameters are shown in Table III. Anisotropic thermal parameters are shown in Table IV. Tables of structure amplitudes (10 pages) have been deposited.[1]

Description of the Structures

All three structures resemble that of $NaVO_3$ and therefore are related to the clinopyroxenes. The structure is based on XO_4 (X = V,P) tetrahedra sharing two vertices to form a single type of chain running parallel to the c-axis (Figs. 1a,b). The C-centering and the twofold symmetry operations generate the other chains to form layers parallel to (100). These layers are separated by one-half of the a-axis and they provide the two types of metal cation sites between them. Using the nomenclature of Burnham *et al.* (*14*) for silicate pyroxenes, the smaller, approximately octahedral site is labeled M1 and the larger, more irregular site is labeled M2. The bridging oxygen in the tetrahedral chain is called O3 and the apical oxygen when viewed along a^* is called O1. Both compounds I and II have sixfold coordinated $M1$ and $M2$ sites lying on a twofold axis, just as α-$NaVO_3$ does. Both sites are occupied by Na in I, and in II the K

TABLE II

SUMMARY OF STRUCTURE REFINEMENTS

	I	II	III
A	1.0	2.0	3.0
B	0.01	0.02	0.03
C	0.00008	0.0005	0.0004
D	300	600	300
g	9.0×10^{-8}	6.0×10^{-8}	2.7×10^{-7}
R	0.035	0.049	0.032
R_w[a]	0.032	0.042	0.039

[a] $R_w = \left[\frac{\Sigma\omega(|F_o| - |F_c|)^2}{\Sigma\omega F_o^2}\right]^{1/2}$.

[1] See NAPS document No. 03229 for 10 pages of supplementary material. Order from ASIS/NAPS c/o Microfiche Publications, P.O. Box 3513, Grand Central Station, New York, New York, 10017, U.S.A. Remit in advance for each NAPS accession number. Institutions and organizations may use purchase orders when ordering, however, there is a billing charge for this service. Make cheques payable to Microfiche Publications. Photocopies are $5.00. Microfiche are $3.00. Outside of the U.S.A. and Canada, postage is $3.00 for a photocopy or $1.50 for a fiche.

TABLE III

POSITIONAL PARAMETERS[a]

Position	Atom[b–d]	x	y	z
8*f*	I[a]	0.29158(5)	0.08864(5)	0.25990(9)
	X II	0.29110(7)	0.08893(8)	0.2528(1)
	III	0.28614(6)	0.08586(7)	0.2240(1)
4*e*	I	0	0.9086(2)	1/4
	*M*1 II	0	0.9104(3)	1/4
	III	0	0.9048(2)	1/4
4*e*	I	0	0.2918(2)	1/4
	*M*2 II	0	0.2980(4)	1/4
	III	0	0.3077(1)	1/4
8*f*	I	0.1299(2)	0.0982(2)	0.1690(4)
	O1 II	0.1280(3)	0.0984(4)	0.1643(6)
	III	0.1254(3)	0.0888(3)	0.1524(5)
8*f*	I	0.3561(2)	0.2416(2)	0.3226(4)
	O2 II	0.3533(4)	0.2448(4)	0.3165(7)
	III	0.3441(3)	0.2364(3)	0.2874(5)
8*f*	I	0.3510(2)	0.0087(2)	0.0336(5)
	O3 II	0.3508(3)	0.0108(4)	0.0248(6)
	III	0.3471(3)	0.0153(3)	−0.0141(5)

[a] Estimated standard deviations in parentheses.
[b] I = $Na(V_{0.66}P_{0.34})O_3$ with $X = 0.658(4)V + 0.342$ P, $M1$ = Na, and $M2$ = Na.
[c] II = $(Na_{0.88}K_{0.12})VO_3$ with X = V, $M1$ = Na, and $M2 = 0.75(3)Na + 0.25$ K.
[d] III = $(Na_{0.5}K_{0.5})VO_3$ with X = V, $M1$ = Na, and $M2$ = K.

TABLE IV

ANISOTROPIC THERMAL PARAMETERS × 10^4[a]

Atom	U_{11}	U_{22}	U_{33}	U_{12}	U_{13}	U_{23}
X I	112(3)	141(3)	129(3)	−16(2)	22(2)	−10(2)
II	129(4)	194(5)	135(4)	−15(4)	41(3)	−3(3)
III	119(3)	154(3)	91(3)	−9(3)	19(2)	−2(2)
*M*1 I	235(9)	230(9)	218(8)	0	45(6)	0
II	174(12)	232(14)	196(12)	0	29(9)	0
III	187(11)	185(11)	181(10)	0	25(9)	0
*M*2 I	441(12)	280(10)	327(10)	0	−63(9)	0
II	275(14)	228(14)	235(14)	0	−90(9)	0
III	311(8)	193(6)	203(6)	0	−36(5)	0
O1 I	209(10)	262(11)	185(9)	−29(9)	32(8)	−1(8)
II	136(14)	303(18)	207(16)	2(13)	38(12)	22(13)
III	146(13)	264(15)	176(12)	21(13)	31(10)	19(12)
O2 I	306(12)	295(12)	291(11)	−108(9)	89(9)	−24(9)
II	268(17)	288(19)	307(19)	−85(15)	76(15)	−21(15)
III	337(18)	191(14)	229(15)	−88(14)	53(13)	−7(10)
O3 I	220(11)	347(13)	421(14)	−6(9)	67(10)	−109(11)
II	209(16)	344(19)	209(16)	−22(14)	64(13)	−64(14)
III	167(14)	268(15)	133(12)	8(12)	38(10)	−39(11)

[a] Estimated standard deviations in parentheses.

TABLE V

BOND GEOMETRY[a,b]

Bond		Distance (Å) I	II	III
*M*1–O1(2)	2×	2.368(2)	2.393(3)	2.386(3)
–O1	2×	2.377(3)	2.392(4)	2.411(4)
–O2	2×	2.303(3)	2.328(4)	2.398(4)
⟨*M*1–O⟩		2.349	2.371	2.398
*M*2–O1	2×	2.407(3)	2.476(5)	2.687(3)
–O2	2×	2.469(2)	2.573(3)	2.818(3)
–O3(5)	2×	2.646(3)	2.667(5)	2.835(3)
–O3(6)	2×			2.946(3)
⟨*M*2–O⟩		2.507	2.572	2.780
X–O1		1.608(2)	1.641(3)	1.642(3)
–O2		1.592(2)	1.628(4)	1.632(3)
–O3		1.764(3)	1.801(4)	1.804(3)
–O3		1.759(3)	1.799(4)	1.808(3)
⟨*X*–O⟩		1.681	1.717	1.722

Bonds	Angle (deg.) I	II	III
O1(2)–*M*1–O1(4)	176.9(1)	176.0(2)	176.9(2)
–O1	90.49(8)	89.7(1)	87.3(1)
–O1(3)	91.87(8)	93.3(1)	90.3(1)
–O2(5)	87.68(8)	86.9(1)	83.1(1)
–O2(7)	90.17(8)	90.4(1)	99.1(1)
O1–*M*1–O1(3)	81.87(9)	82.3(2)	80.6(1)
–O2(5)	174.1(1)	173.1(1)	169.5(1)
–O2(7)	92.53(8)	91.9(1)	95.0(1)
O2(5)–*M*1–O2(7)	93.1(1)	94.1(2)	90.8(2)
O1–*M*2–O1(3)	80.7(1)	78.9(2)	70.9(1)
–O2(6)	83.35(8)	82.8(1)	82.63(9)
–O2(8)	85.45(8)	83.1(1)	82.74(9)
–O3(5)	141.90(8)	140.0(1)	136.51(8)
–O3(7)	113.41(7)	114.5(1)	117.81(8)
–O3(6)			92.21(9)
–O3(8)			160.0(1)
O2(6)–*M*2–O3(5)	131.0(1)	134.2(2)	138.7(1)
–O3(7)	62.77(8)	63.0(1)	58.53(9)
–O2(8)	165.3(1)	161.7(2)	162.0(1)
–O3(6)			106.24(9)
–O3(8)			84.73(9)
O3(5)–*M*2–O3(5)′	78.08(9)	80.3(2)	85.92(9)
O1–*X*–O2	110.6(1)	109.4(2)	110.3(2)
–O3	110.7(1)	110.9(2)	110.6(1)
–O3(4)	111.6(1)	111.2(2)	110.8(2)

TABLE V (*cont.*)

Bonds	Angle (deg.) I	II	III
O2–*X*–O3	109.7(1)	110.2(2)	110.5(2)
–O3(4)	105.4(1)	105.9(2)	106.8(1)
O3–*X*–O3(4)	108.6(1)	109.1(2)	107.8(1)
O3(4)–O3–O3(4)′	173.4(1)	171.9(2)	168.0(2)

[a] The position of an atom $A(n)$ is derived from that of A shown in Table III by the nth symmetry operation as appears in the "International Tables for X-Ray Crystallography," Vol. I (1965) for the space group $C2/c$. For example, O1(2) is related to O1 by the symmetry operation, $\bar{x}, \bar{y}, \bar{z}$.

[b] Estimated standard deviations in parentheses.

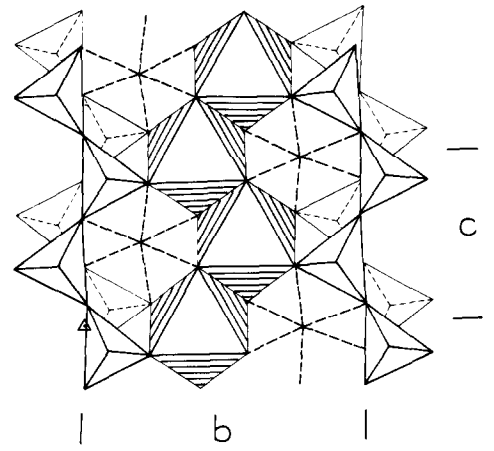

1A

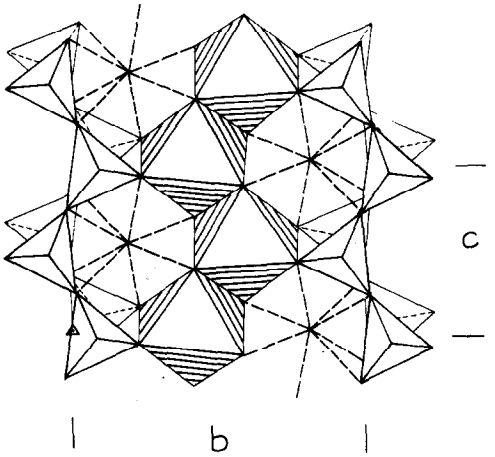

1B

preferentially occupies the larger $M2$ sites with the Na taking up all the $M1$ sites and the rest of the $M2$ sites. The bond geometry of these three compounds is shown in Table V. The average $M1$–O distance increases slightly from 2.349 to 2.371 Å from I to II. The $M2$–O bonds range from 2.407 to 2.646 Å in I and from 2.476 to 2.667 Å in II. At the same time, the distance of M2 to the next nearest oxygen atoms (O3(6)) decreases from 3.183 Å in I to 3.151 Å in II, but this latter distance is still too large to allow these oxygens to be included in the $M2$ coordination polyhedron. Compound III, however, adopts the true diopside structure with the Na and K ordered into $M1$ and $M2$ sites, respectively. The $M2$–O distance averaged over the six nearest neighbors has increased to 2.780 Å while the $M2$–O3(6) distance has decreased to 2.946 Å so that the $M2$ site may now be considered to be eight-fold coordinated, as in diopside (15).

There is only a small, perhaps insignificant, change in the average V–O distance from II to III. The short $\langle X\text{–}O \rangle$ distance of 1.681 Å in I undoubtedly reflects the substitution of P for V in one-third of the tetrahedral sites. There is

FIG. 1. Structures of metavanadate clinopyroxenes projected on the *bc* plane, (a) $Na(V_{0.66}P_{0.34})O_3$ and $(Na_{0.88}K_{0.12})VO_3$; (b) $(Na_{0.5}K_{0.5})VO_3$. Unit cell origin is indicated by △. Side faces of $M1$ octahedra are shaded and the coordination of $M2$ polyhedra is shown by heavy broken lines.

no evidence of any ordering between V and P. In all three cases, the distance of X to the bridging oxygen O3 is about 0.16 Å longer than those to the nonbridging ones, a characteristic feature of these corner-shared XO_4 tetrahedral chains. The fact that two more oxygen atoms enter into the coordination polyhedron of $M2$ in III has little effect on the V–O distances.

Discussion

The effects of cation substitution in the alkali metal metavanadate clinopyroxenes may be discussed in the light of structural data obtained in the present study and previous studies on $LiVO_3$ and α-$NaVO_3$. The data reported by Marumo *et al.* (*4*) on α-$NaVO_3$ were used here since their refinement seems to be the most satisfactory. Data pertinent to this discussion are summarized in Table VI.

Beginning with $LiVO_3$ and ignoring the P substituted $NaVO_3$ for the moment, the most obvious effect of placing a larger cation in the $M2$ site is an increase in the size of that site. This is shown by a progressive increase in the average $M2$–O distance from 2.284 Å in $LiVO_3$ to 2.780 Å in III. The average $M1$–O distance increases only slightly from α-$NaVO_3$ to III as the K is found to occupy preferentially the $M2$ site. The remarkably constant dimension of the VO_4 tetrahedron across the series has been noted. This is quite contrary to the silicate clinopyroxenes where the average of the two Si–O bridging bond lengths $\langle Si\text{–}O\rangle_{br}$ was found to be highly correlated to both r_{M1} and r_{M2}, the effective ionic radii of $M1$ and $M2$ (*16*). Thus while $\langle Si\text{–}O\rangle_{br}$ varies between 1.62 and 1.65 Å among the Li and Na $C2/c$ silicate pyroxenes, $\langle V\text{–}O\rangle_{br}$ only varies between 1.800 and 1.808 Å among the metavanadate analogs. This suggests that the $(VO_3)_\infty$ chains are even more rigid than the $(SiO_3)_\infty$ chains. Two simultaneous movements of this rigid chain can be shown to result from the expansion of the $M2$ site in order to accommodate a larger cation. These are the rotations of the tetrahedra to adopt a different chain configuration and the so-called back-to-back displacement of the chain in the c-direction.

Three distinct configurations of the silicate chains in pyroxenes have been defined by Thompson (*17*) and by Papike *et al.* (*18*). Beginning with an extended or E chain, where the chain angle measured by the angle O3–O3(4)–O3′ is 180° (Fig. 2), each tetrahedron can be rotated about an axis normal to the layers and passing through the apical oxygen O1 which links the tetrahedron to two $M1$ octahedra. If the triangular face normal to this axis is oriented similarly to the nearest parallel

TABLE VI

SOME STRUCTURAL DATA FOR ALKALI METAVANADATE CLINOPYROXENES

	$LiVO_3$	α-$NaVO_3$	I	II	III
$\langle M1\text{–}O\rangle$ (Å)	2.153	2.364	2.349	2.371	2.398
$\langle M2\text{–}O\rangle$ (Å)	2.284	2.513	2.507	2.572	2.780
$\langle X\text{–}O\rangle$ (Å)	1.725	1.723	1.681	1.717	1.722
$\langle X\text{–}O\rangle/\langle M2\text{–}O\rangle$	0.755	0.685	0.671	0.667	0.619
Δ(Å)[a]	1.927	1.435	1.324	1.238	0.625
β (deg.)	110.48	108.47	107.62	107.56	104.17
ϕ (deg.)[b]	−19.2	5.5	6.6	8.1	12.0
δ-ϵ (deg.)[b]	−8.1	2.6	3.1	3.9	5.9

[a] Tetrahedral chain displacement = $2[Cz_{03} - a\cdot\cos\beta(0.5 - x_{03})]$, Ref. (*1*).

[b] A negative value indicates S rotation.

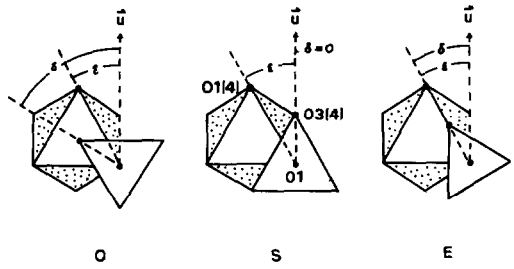

FIG. 2. Schematic representation of idealized *E*-, *O*-, and *S*-chain configurations.

faces of the two octahedra sharing this oxygen, the chain is termed *S* rotated (Fig. 2). Rotation in the opposite sense will result in oppositely oriented faces or an *O*-rotated chain. The chain angle for the idealized and completely *S*- or *O*-rotated chain will be 120°. It is proposed here to define the chain configuration quantitatively by determining the orientations of these octahedral and tetrahedral faces with respect to the *c*-direction in the *C*2/*c* clinopyroxene structures. The criterion used is illustrated in Fig. 2. The angle ε is subtended by the O1–O1(4) edge of the *M*1 octahedron and a unit vector **u** parallel to the *c*-axis. The angle δ is subtended by **u** and the projection of the O1–O3(4) edge of the tetrahedron on the *bc* plane. O1(4) and O3(4) are related to O1 and O3 by the *c*-glide operation. The angle δ–ε is then 0° for *E*, +30° and −30° for completely rotated *O* and *S* chains, respectively. For real structures δ–ε varies between +30° and −30°, and together with ϕ (= 180° − ∠O3–O3(4)–O3′) is a measure of the tetrahedral chain rotation. It was pointed out by Hawthorne and Calvo (*1*) that the metavanadate orthopyroxenes all had *E* chains, while Table VI shows that all the known metavanadate clinopyroxenes have O chains except $LiVO_3$, which has an *S* chain. The correlation between ⟨*M*2–O⟩ and δ–ε as shown in Table VI is immediately obvious, i.e., increasing the size of the *M*2 cation results in an increased amount of *O* rotation. This is consistent with the conclusion of Papike *et al.* (*18*) for the silicate pyroxenes. However, a sixfold coordination for *M*2 does not necessarily lead to an *S* rotation, as it was pointed out by Hawthorne and Calvo (*1*), since III is the only compound with *O* chains in this series to have an eightfold coordinated *M*2 site. It can also be seen from Fig. 2 that increasing the amount of *O* rotation should lead to an increase in the *b*-axis and a decrease in the *c*-axis. Indeed, the *b*-axis increases from 9.468 Å in α-$NaVO_3$ to 9.997 Å in III with a smaller decrease in *c* from 5.879 to 5.804 Å.

The ratio of the tetrahedral edge to the *M*1 octahedral edge is 1:1 for a completely rotated chain and is $3^{1/2}$:2 for an extended chain. Since the size of the tetrahedron is hardly affected by changing the size of the metal cation in the structure, rotation of the chain from say *E* to *O* configuration would lead to structural misfit between the tetrahedral and octahedral layers if chain rotation were the only mechanism by which the structure modifies itself to accommodate this change. This was first realized by Cameron *et al.* (*19*) for the effect of thermal expansion on some silicate pyroxenes. A concomitant displacement of the tetrahedral chain then becomes necessary to correct for this misfit. This second chain movement can be shown to be the "back-to-back" displacement described by Hawthorne and Grundy (*20*). It is the relative displacement Δ in the *c*-direction of the chains in adjacent layers, measured by the separation of the mid-points of the O3–O3(4) tetrahedral edges projected onto the *bc* plane. Table VI shows that this displacement Δ decreases progressively from 1.927 Å in $LiVO_3$ to 0.625 Å in $(Na_{0.5}K_{0.5})VO_3$. Since the two chains in question are related by a twofold rotation in the *C*2/*c* structure, a decrease in chain displacement should be accompanied by a reduction in β. A progressive decrease in β from $LiVO_3$ to III can be seen from Table VI.

When the parameters measuring chain rotation and displacement, i.e., ϕ, δ–ε, Δ, and β, are plotted against ⟨*M*2–O⟩, the points corresponding to the P-substituted $NaVO_3$ invariably fall off the otherwise smooth curves. It may be noted from Table VI that while there

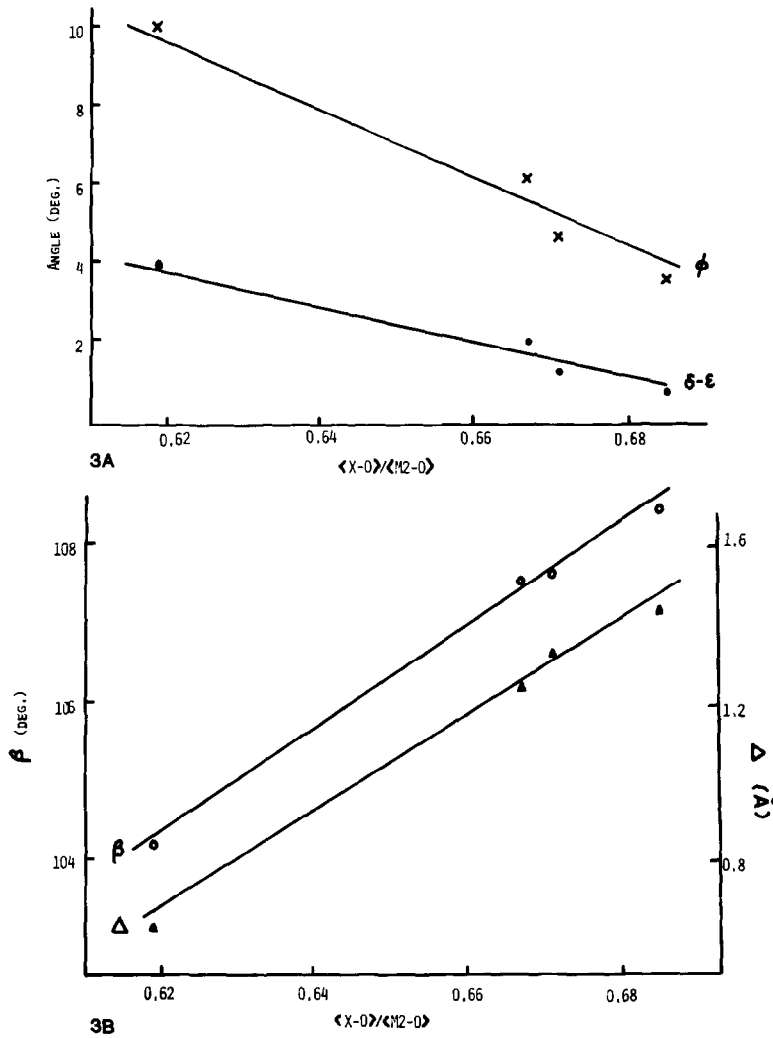

FIG. 3. Correlation between $\langle X\text{–O}\rangle/\langle M\text{–O}\rangle$ and (a) chain rotation parameters ϕ and δ–ε; (b) chain displacement parameters Δ and β.

is an insignificant decrease in $\langle M2\text{–O}\rangle$ from $NaVO_3$ to $Na(V_{0.66}P_{0.34})O_3$, there are significant changes in the above four parameters. The trend that these changes follow suggests that decreasing $\langle X\text{–O}\rangle$ produces the same effect on the structure as increasing $\langle M2\text{–O}\rangle$ does. Therefore a strong correlation between the ratio $\langle X\text{–O}\rangle/\langle M2\text{–O}\rangle$ and the amount of chain rotation and displacement is expected. Figures 3a,b show this correlation for α-$NaVO_3$ and the three compounds studied in this work, all of which feature an O-rotated chain and an $M1$ site exclusively occupied by Na. The relationship between $\langle X\text{–O}\rangle/\langle M2\text{–O}\rangle$ and Δ, β, ϕ, and δ–ε is almost linear in each case. This is in apparent contradiction to the conclusion reached by Ribbe and Prunier (*16*) that in the silicates a shorter $\langle$Si–O3$\rangle$ length is accompanied by decreased O rotation. However, it must be noted that with the silicates the shorter $\langle$Si–O3$\rangle$ is a result of smaller r_{M1} and r_{M2}. In the present case with the metavanadates, the shorter $\langle X\text{–O}\rangle$ is a direct result of chemical constraint on the

tetrahedral cation which, although hardly affects $\langle M2\text{–}O\rangle$, results in a significantly longer $M2$–O3 bond length which increases from 2.611 Å in a α-$NaVO_3$ to 2.646 Å in $Na(V_{0.66}P_{0.34})O_3$. This weakened $M2$–O3 interaction may be directly responsible for the amount of chain rotation in the more rigid $(VO_3)_\infty$ chain.

The approximate linearity in the correlations shown above could not be extended to include $LiVO_3$. While the present study shows the effects of varying r_{M2} on the tetrahedral chain rotation and displacement, the effects of varying r_{M1} are much less understood. Although the chain configuration changes from S in $LiVO_3$ to O in α-$NaVO_3$, an intermediate phase between $LiVO_3$–$NaVO_3$ may or may not have an E-chain configuration since the extended chain seems to be characteristic of the metavanadate orthopyroxenes. A study of the system $(Li,Na)VO_3$ is now in progress so that a more direct comparison with the analysis of Ribbe and Prunier (*16*) on the silicates can be made.

Acknowledgments

The work has been supported by the National Research Council of Canada through an operating grant. We would like to thank Dr. F. C. Hawthorne for helpful discussions.

References

1. F. C. HAWTHORNE AND C. CALVO, *J. Solid State Chem.* **22**, 157 (1977).
2. M. GANNE, Y. PILFARD, AND M. TOURNOUX, *Canad. J. Chem.* **52**, 3539 (1974).
3. C. T. PREWITT, A. SACROUG, S. SUENO, AND M. CAMERON, *Geol. Soc. Amer. Abs. Prog.* **4**, 630 (1972).
4. F. MARUMO, M. ISOBE, AND S. IWAI, *Acta Crystallogr. B* **30**, 1628 (1974).
5. K. RAMANI, A. M. SHAIKH, B. S. REDDY, AND M. A. VISWAMITRA, *Ferroelectrics* **9**, 49 (1975).
6. R. D. SHANNON AND C. CALVO, *Canad. J. Chem.* **51**, 265 (1973).
7. S. SAWADA AND S. NOMURA, *J. Phys. Soc. Japan* **6**, 192 (1951).
8. M. MATSUDA, *J. Phys. Soc. Japan* **36**, 759 (1974).
9. A. G. BERGMAN AND Z. I. SANZHAROVA, *Russ. J. Inorg. Chem.* **15**, 877 (1970).
10. S. OHASHI, "Topics in Phosphorus Chemistry" (M. Grayson and E. J. Griffith, Eds.), Vol. I, Wiley, New York (1964).
11. J. PERRAUD, *Rev. Chim. Miner.* **11**, 302 (1974).
12. M. P. GLAZYRIN, *Dokl. Akad. Nauk SSSR* **221**, 91 (1975).
13. A. C. LARSON, *Acta Crystallogr.* **23**, 664 (1967).
14. C. W. BURNHAM, J. R. CLARK, J. J. PAPIKE, AND C. T. PREWITT, *Z. Kristallogr.* **125**, 109 (1967).
15. B. WARREN AND W. L. BRAGG, *Z. Kristallogr.* **69**, 168 (1929).
16. P. H. RIBBE AND A. R. PRUNIER, *Amer. Mineral.* **62**, 710 (1977).
17. J. B. THOMPSON, *Amer. Mineral.* **55**, 292 (1970).
18. J. J. PAPIKE, C. T. PREWITT, S. SUENO, AND M. CAMERON, *Z. Kristallogr.* **138**, 254 (1973).
19. M. CAMERON, S. SUENO, C. T. PREWITT, AND J. J. PAPIKE, *Amer. Mineral.* **58**, 594 (1973).
20. F. C. HAWTHORNE AND H. D. GRUNDY, *Canad. Mineral.* **15**, 50 (1977).